

**Supporting Information**

**Design of Dual Stimuli Responsive Polymer Modified Magnetic Nanoparticles for Targeted Anti-Cancer Drug Delivery and Enhanced MR Imaging**

Dipsikha Bhattacharya<sup>\*a,c</sup>, Birendra Behera<sup>b</sup>, Sumanta Kumar Sahu<sup>d</sup>, Rajakumar Ananthakrishnan<sup>a</sup>, Tapas Kumar Maiti<sup>b</sup> and Panchanan Pramanik<sup>\*a</sup>

Department of Chemistry, Indian Institute of Technology Kharagpur<sup>a</sup>, West Bengal, India.

Department of Biotechnology, Indian Institute of Technology Kharagpur<sup>b</sup>, West Bengal, India.

Nanotherapeutics Laboratory, CSIR-Indian Institute of Toxicology Research<sup>c</sup>, Lucknow, India.

Department of Chemistry, Indian School of Mines, Dhanbad, India<sup>d</sup>

Corresponding author. E-mail: dipsikha.chem@gmail.com, pramanik1946@gmail.com; Phone no: +91-522-2620107, Fax no: +91-522-2628227.

**Table S1:** Hydrodynamic sizes, Poly dispersity index (PDI), and Zeta Potential values of **1** and **2**.

SI. No	MFNPs Modifications	Hydrodynamic Sizes at pH 7.4	Poly Dispersity Index (PDI)	Zeta Potential (mV) at pH 4	Zeta Potential (mV) at pH 7.4
1	Poly-MFNPs (1)	80±10	0.213	45.5±0.9	14.5±1.22
2	FA-Poly-MFNPs (2)	91±5	0.256	35.5±1.7	-12.2±0.17

**Detailed description of DLS and Zeta potential analysis:**

The uniform hydrodynamic sizes of these Poly-MFNPs (**1**) were observed around 80±10 nm (PDI-0.213) reflecting good stabilization of these polymer stabilized MNPs. The  $\zeta$  potential of **1** gradually increased from 14.5mV to 45.5mV with decreasing pH (7.4 to 4.5) reflecting the successful modification with  $-NH_2$  groups of the polymer. (Table S1) The successful conjugation of **1** with folate functionalities was also verified by DLS and Zeta potential analysis. It was clear from the HD values that there is a little increase in sizes (91±5 nm) for FA-Poly-MFNPs (**2**) compared to Poly-MFNPs (80 nm) at pH 7.4. And for zeta potential analysis, these

FA-Poly-MFNPs showed positively charged surface (35.5 mV at pH 4.5) while with increasing pH, their increased negative potential values (-12.2 mV at pH 7.4) and (-19.6 mV at pH 9) confirmed their successful modification of carboxyl groups of FA. Therefore, it could be assumed that Poly-MFNPs contain reasonable number of amine functionalities which are replaced with functional carboxyl groups deciphering conjugation with FA, which was also confirmed TNBS analysis. Therefore, these Poly-MFNPs lost some of the amine groups with the occurrence of carboxyl groups, which can offer possibility of enhanced water solubility as well as superior hydrogen bonding tendency with surrounding surface water molecules.<sup>1</sup>

**Table S2:** TNBS assay showing quantity concentration and number of amine and folate groups present on the nanoparticles.

SI. No	Modified MFNPs	Functional end groups	Surface amine density ( $\mu\text{mol}/\text{mg}$ )	Concentration of functionalized groups ( $\mu\text{mol}/\text{mg}$ )	Number of functionalized groups
1	Poly-MFNP(1)	-NH <sub>2</sub>	1.4	1.4	1080 (-NH <sub>2</sub> )
2	FA-Poly-MFNPs (2)	-FA	0.3	1.1	830 (-COOH)

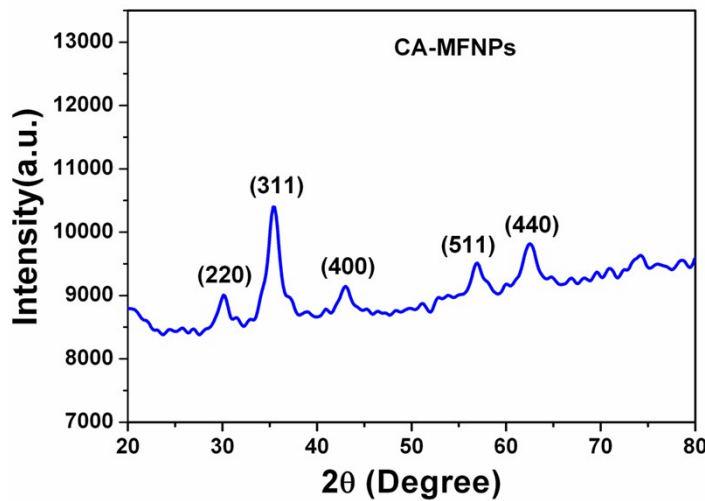


**Figure S1.** XRD pattern of citrate stabilized mixed ferrite nanoparticles (CA-MFNPs).

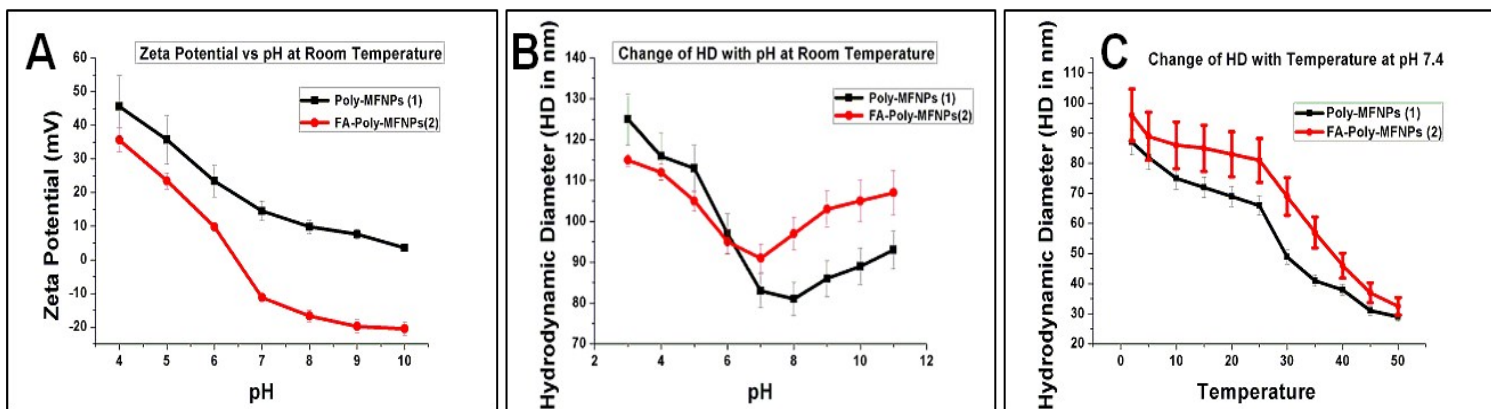


**Figure S2.** (A) Change of Zeta Potential values of Poly-MFNPs (1) and FA-Poly-MFNPs (2) with pH at 25°C. (B) pH-responsive transition of the hydrodynamic diameter 1 and 2 at 25°C. (C) Temperature responsive transition of the hydrodynamic diameter 1 and 2 at physiological pH (7.4).

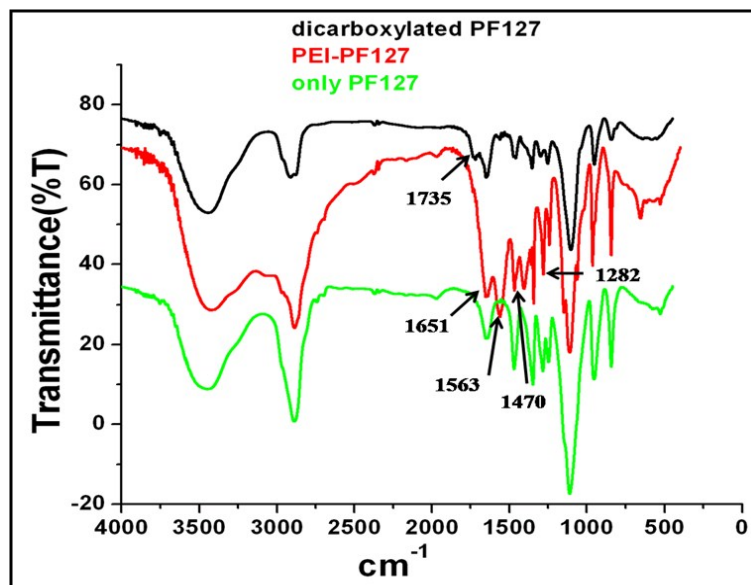


**Figure S3.** FT-IR spectra of the synthesized polymers i.e dicarboxylated PF127 and PEI-PF127 as well as PF127 (taken as received).

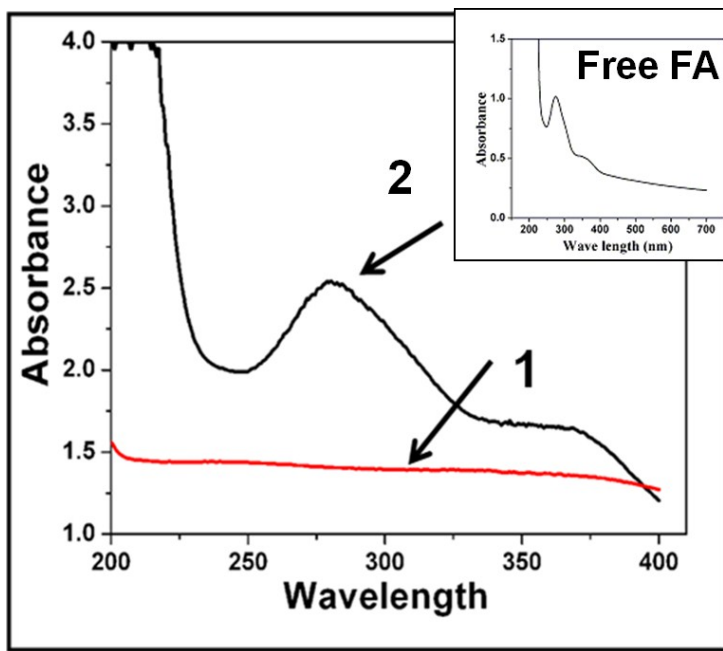


**Figure S4.** (a) UV-Vis spectra of Poly-MFNPs (**1**) and FA-Poly-MFNPs (**2**).

#### TGA analysis:

From TGA graphs, Poly-MFNPs (**1**) showed ~50% of weight loss with increasing temperature, which was quite clear compared to CA-MFNPs assuming due to the surface modification with copolymer molecules. To further confirm the modification with PEI-PF127 and FA, amine functionalities present on the surface of Poly-MFNPs (**1**) and FA-Poly-MFNPs (**2**) were checked by TNBS assay. (Data given in Table S2) The results confirmed the stepwise reduction in the amine group concentration on nanoparticle surface is the confirmation of modification by block copolymer and folic acid.

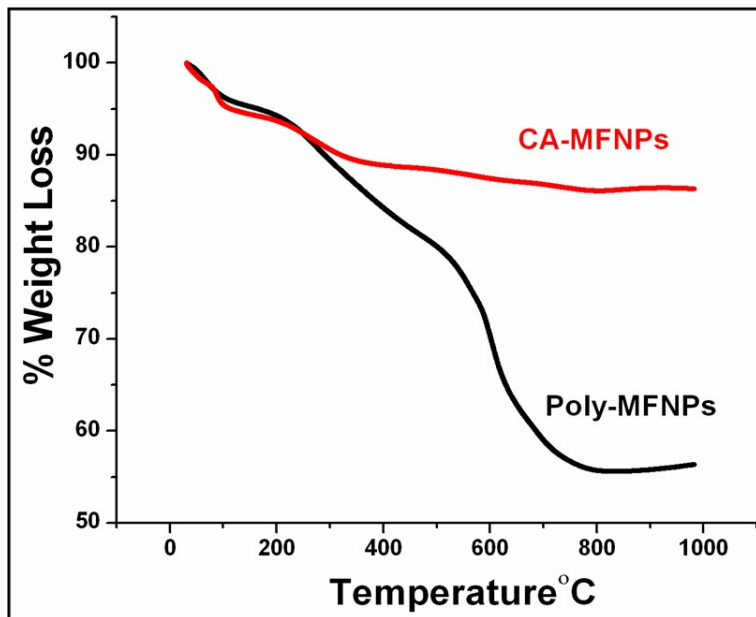


**Figure S5:** Thermo gravimetric analysis (TGA) curves of CA-MFNPs and Poly-MFNPs (**1**).

#### VSM analysis:

To authenticate the feasibility and sensitivity of Poly-MFNPs (**1**) as enhanced MR imaging nanoprobes, it is crucial that MFNPs should retain their favourable magnetic properties after surface modification with biomolecules. The magnetic properties of CA-MFNPs, Poly-MFNPs and FA-Poly-MFNPs have been evaluated using VSM analysis and the results authenticated that all these MFNPs exhibited complete superparamagnetism without hysteresis, coercivity, and remanence at room temperature. The magnetization value observed for the CA-MFNP crystals was 63.6 emu/g while for Poly-MFNPs (**1**), the magnetization value was 49.66 emu/g respectively. The lower saturation magnetization values of **1** compared to CA-MFNPs could be attributed due to the presence of nonmagnetic organic components, which can reduce the total magnetization to a different extent signifying the successful surface modification of these

MFNPs.<sup>2</sup> There is no obvious loss of saturation magnetization observed after folic acid conjugation compared with that of **1** as reflected in **2**.

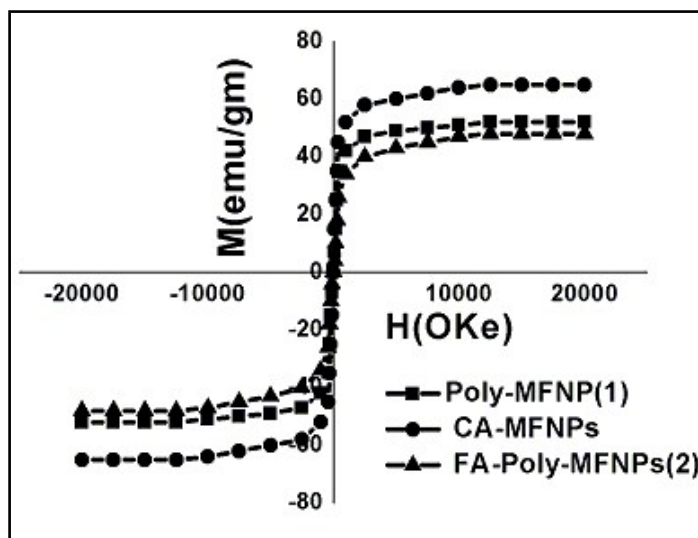


**Figure S6:** Plots of magnetization versus magnetic field at 300 K for CA-MFNPs, Poly-MFNPs (1) and Poly-FA-MFNPs (2).

### XPS Analysis

XPS analysis is a useful method for the determination of different elements along with their chemical state. High resolution XPS spectra analysis (shown in **Figure S7**) has been further performed to validate the successful coating of PEI-PF127 followed by FA on ferrite surface. Taking 284.2 eV as standard for bulk C1S, the broad shoulder can be fitted into three peaks 285.68, 285.18, 284.83 eV, attributing to -C-N, -C-O and C-C groups in the nanoconjugates **1**. For C 1S of FA-PEI-PF127-MFNP (**2**), considering 285 eV as standard, the broad shoulder are deconvoluted into four peaks at 284.93, 285.17, 285.56 and 287.74 that can be attributed to -C-C-, -C-O, -C-N and -NH-C=O groups, respectively.<sup>3</sup> The high resolution N1S spectrum of **1** exhibits a broad shoulder at 399.6 eV (N-H) corresponding to the presence of free amine groups of PEI-PF127 on the surface<sup>4</sup> whereas in **2**, the N 1S displays two peaks at 399.3 eV and 401.6 eV, corresponding to the free -NH<sub>2</sub> groups of PEI-PF127 ligand and amide (-NH-C=O) bonding within the FA structure and also the amide linkage between FA and nanoparticle surface. The

presence of  $Mn^{2+}$  is confirmed by the presence of The  $Mn2p3/2$  and  $Mn2p1/2$  doublet with binding energy values of 640.2 and 651.97 validating the presence of Mn-O bonds in the sample. The  $Fe2p$  doublet with binding energy values of 710.8 and 724.29 eV authenticates the presence of Fe–O bonds, typical for magnetite.

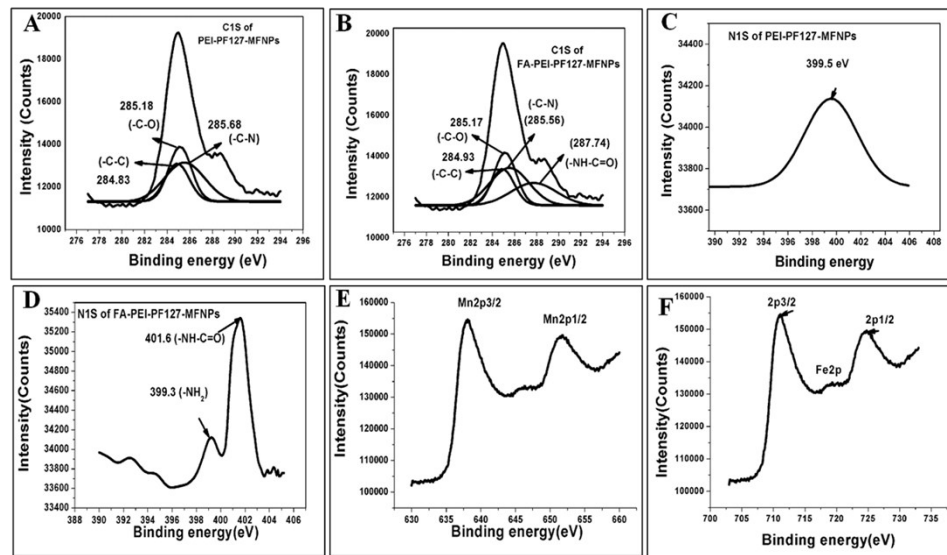


**Figure S7.** XPS spectrum of A) and B) C1s of Poly-MFNP and FA-Poly-MFNPs. C) and D) N1s of Poly-MFNP and FA-Poly-MFNPs. E) Fe2p F) Mn2p of Poly-MFNPs.

#### MTT Assay

These **1** and **2** nanoparticles without DOX loading caused no cytotoxic effect on both the HeLa and HaCaT cells exhibiting cell viability of almost 85% on treatment with 200 $\mu$ g/mL. Hence these nanoparticles were safe and could be used for biomedical purposes.

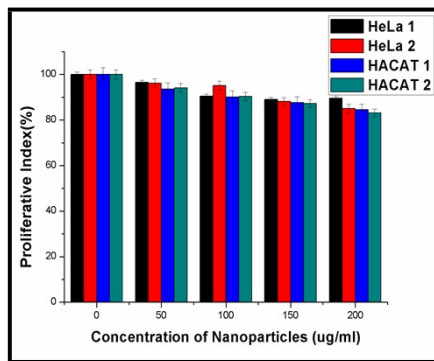


**Figure S8.** (a) Cell viability assays of Poly-MFNP (**1**) and FA-Poly-MFNP (**2**) in HeLa and HaCaT cell lines.

### **Intracellular Uptake of RITC-labeled Poly-FA-MNPs in HaCaT and HeLa cells**

To further corroborate the receptor targeting ability of RITC-labelled Poly-FA-MNPs (**3**) towards FR (+) HeLa cells (HeLa-HFAR), the cellular internalization of these nanoparticles was also cross verified using FR (+) HeLa and FR (-) HaCaT cells for 4h. The differential uptake behaviour of both the types of cells was well evidenced from fluorescence images [Shown in Figure S9(A-B)]. It is clearly observed that these particles has been selectively accumulated on the surface of the FR (+) HeLa cells as compared to FR (-) HaCaT cells, signifying their preferential internalization to HeLa cells through receptor mediated endocytosis. Hence, these results clearly confirmed that these RITC-conjugated nanoparticles (**3**) could be able to selectively internalize via folate receptor mediated endocytosis.

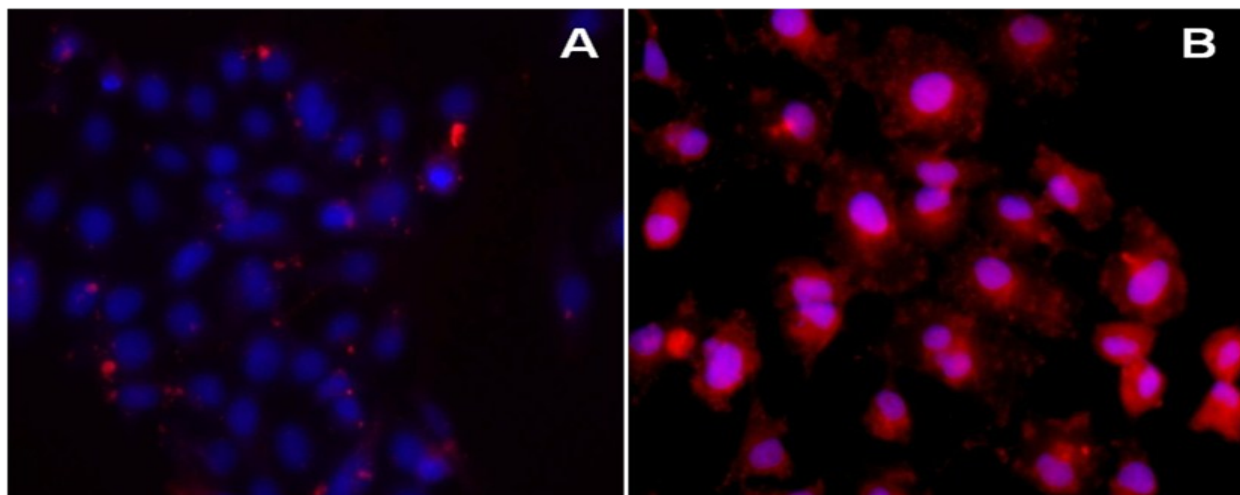


**Figure S9(A-B):** Comparison of intracellular uptake of (A) HaCaT normal fibroblast cells treated with RITC-FA-Poly-MFNPs. (B) HeLa cells treated with RITC-FA-Poly-MFNPs.

### **Intracellular Uptake of RITC-labeled Poly-FA-MNPs in presence and in absence of free FA**

In order to revalidate the ambiguous uptake in presence of free FA, the intracellular uptake of **3** in presence and in absence of FA have been cross verified in HeLa cells using fluorescence imaging analysis. In absence of free FA in medium, **3** are easily penetrated into HeLa cells and exhibit bright red fluorescence near the nucleus (Figure S10 (B)) while in presence of FA,

although there is some uptake, but the amount of uptake has been significantly reduced. (Figure S10 (A)) From these data, the FA mediated receptor-mediated internalization of **2** to cancer cells has been corroborated.

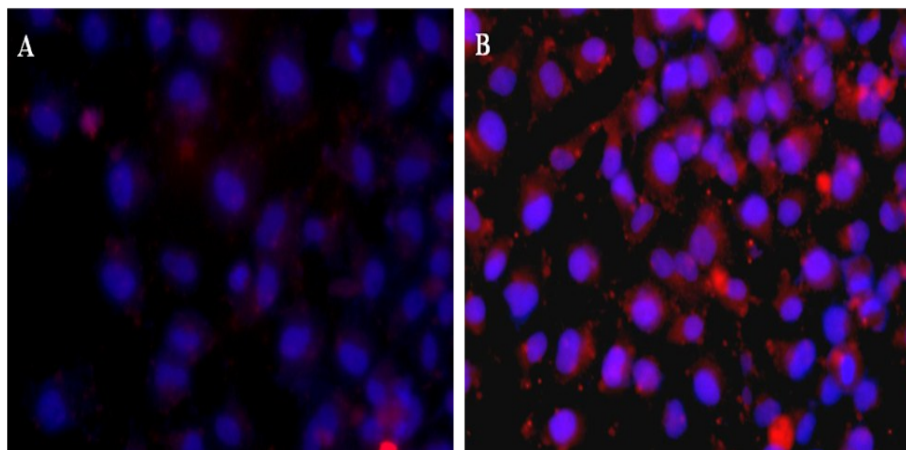


**Figure S10.** Fluorescence images of HeLa cells incubated RITC labelled FA-Poly-MFNPs (**3**) A) In presence of free FA and B) In absence of free FA.

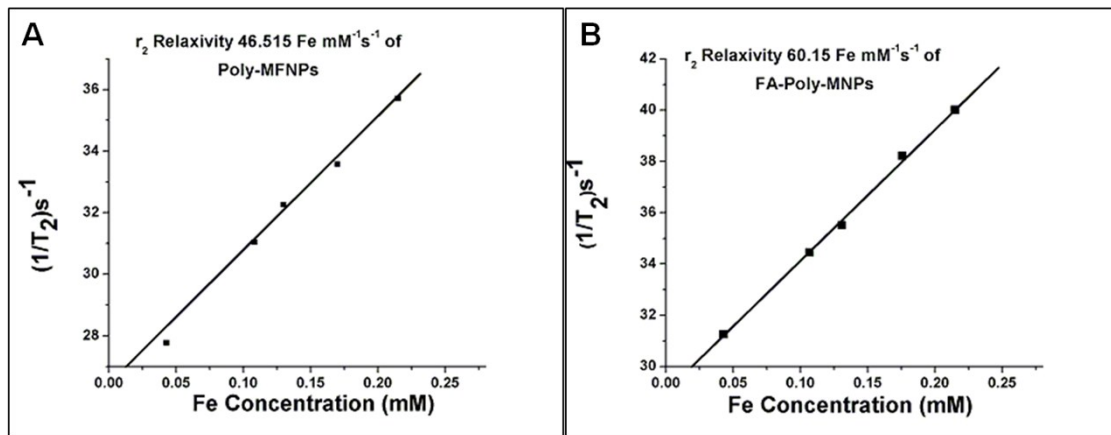


**Figure S11.**  $r_2$  relaxivity values of Poly-MFNPs and FA-Poly-MNPs in HeLa-HFAR cells.

**Figure S12. Details of  $^1\text{H}$  NMR spectra of dicarboxylated PF127 and PEI-PF127.**

$^1\text{H}$  NMR spectra of dicarboxylated PF127 (400 MHz,  $\text{D}_2\text{O}$ , TMS) showed the peaks at  $\delta$  2.55–2.65 ppm (methylene protons  $-\text{CH}_2-\text{CH}_2-$  of succinic group),  $\delta$  4.2 (OCH<sub>2</sub>CH<sub>2</sub>OCO) (ppm), 1.05 (d, 3H,  $-\text{CH}_3$  of PPO), 3.3–3.8 (m, 3H, 4H,  $-\text{CH}_2\text{CHO}-$  of PPO and  $-\text{CH}_2\text{CH}_2\text{O}-$  of PEO),

8.14, 7.43, and 7.06 (1H, imidazole).  $^1\text{H}$  NMR spectra of PEI-cross-linked PF127 (400 MHz,  $\text{D}_2\text{O}$ , TMS) showed the peaks at  $\delta$  (ppm)  $\sim$  2.55-2.65 ppm (methylene protons  $-\text{CH}_2\text{CH}_2-$  of succinic group),  $\delta$  (ppm)  $\sim$  1.05 (, 3H,  $-\text{CH}_3$  of PPO),  $\delta$  (ppm)  $\sim$  2.3-2.9 (methylene and methane protons groups of PEI), 3.2–3.7 (m, 3H, 4H,  $-\text{CH}_2\text{CHO}-$  of PPO and  $-\text{CH}_2\text{CH}_2\text{O}-$  of PEO).

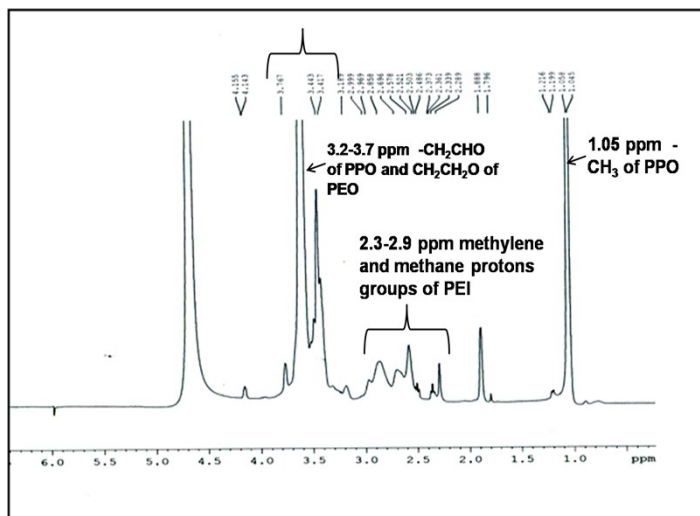
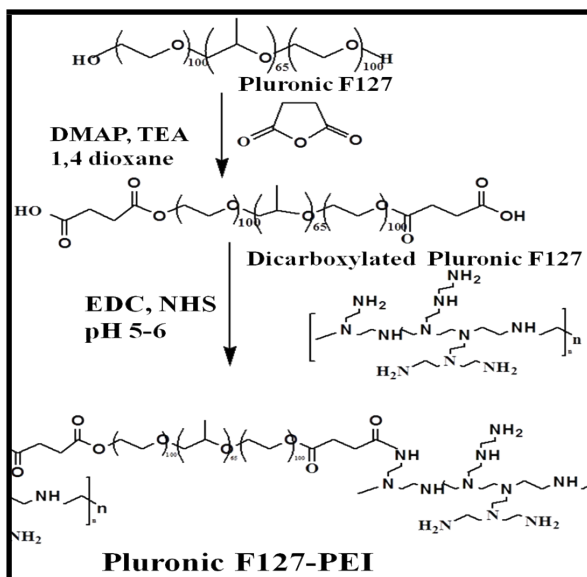


**Figure S12:**  $^1\text{H}$  NMR spectrum of PEI crosslinked PF127; 400 MHz,  $\text{D}_2\text{O}$



**Scheme S1:** Schematic illustration of the synthesis of PEI-PF127 blocks copolymer.

**References:**

1. J. DeRuiter. Principles of Drug Action 1, Spring 2005, Carboxylic Acids Part 1.
2. D. Bhattacharya, M. Das, D. Mishra, I. Banerjee, S. K. Sahu, T. K. Maiti and P. Pramanik. *Nanoscale*, 2011, **3**, 1653.
3. S. Wang, Y. Zhou, H. Niu and X. Zhang, *Curr. Appl. Phys* 2011, **11**, 1337.
4. N. S. Baek, J. H. Lee, Y. H. Kim, B. J. Lee, G. H. Kim, I. H. Kim, M.A. Chung and S.D. Jung, *Langmuir* 2011, **27**, 2717.